Study of the Influence of Atrial Dilatation on the Development of Atrial Fibrillation Through Its Modeling

Luisa M Gavier[1], Violeta Puche-García[1], Marcos Latorre[1], Javier Saiz[1]

[1]Centro de Investigación e Innovación en Bioingeniería, Universitat Politècnica de València, Valencia, Spain

Abstract

Atrial stretching and subsequent dilatation are early markers of hypertensive heart disease (HHD), a condition characterized by slow left atrial (LA) structural and electrical remodeling that increases the risk of arrhythmias. This study aims to investigate the development of atrial fibrillation (AF) episodes through coupled modeling of electrical activity with both elastic and growth and remodeling (G&R) responses.

Electrophysiological activity was simulated using the Courtemanche model on different 3D LA patches of adjusted dimensions according to the states of acute stretch and chronic dilatation under study. Different conductance parameters were employed to reproduce the healthy and persistent AF (peAF) electrical conditions, considering in turn the effect of the stretch-activated channels (SACs).

The study of the vulnerable window (VW) and the frequency of cardiac arrhythmia generation unveiled a greater vulnerability to the development of AF and a higher re-entrant activity when it comes to an atrial tissue with peAF along with SACs in an acutely stretched state. In a chronically dilated atrial tissue, an increased vulnerability to the development of AF was also observed, with a higher VW as the state of severity of chronic dilation progresses.

1. Introduction

Hypertensive heart disease (HHD) is a condition that arises as a result of elevated blood pressure and represents a major risk factor for cardiovascular disease (CVD) morbidity and mortality. In recent years, it has become the second leading cause of heart failure, resulting in an estimated 0.85 million deaths worldwide in 2019 [1,2].

Left atrial (LA) structural and functional alterations are an early sign of HHD, being a useful index of cardiovascular risk and disease burden. Growth and remodeling (G&R) atrial response constitutes a time-slowed adaptative process to myocardial stress associated with persistent hypertension and whose primary purpose is to maintain tissue homeostasis [2]. In the short-term, reversible adaptation occurs through atrial stretching, leading to the activation of the stretch-activated channels (SACs) and the consequent alteration of Ca^{2+} transients [3]. In chronic hypertension, the compensatory tissue response becomes an irreversible process of G&R that results in the development of myocardial fibrosis and the increase in size of individual cardiomyocytes. The ensuing altered myocardial architecture with consequent conduction abnormalities, provides the structural substrate for intra-atrial reentrant circuits development and atrial fibrillation (AF) maintenance. LA enlargement along with the progression of HHD result in LA systolic dysfunction and LA dilation, also associated with a higher risk of AF [2].

In this study, atrial myocyte electrical model and both hyperelastic and G&R mathematical models are employed to simulate, through six 3D atrial-tissue models, LA function and response to acute stretch and two specific chronic dilatation states in a finite element solver. The aim is to investigate the vulnerable window (VW) and dominant frequency (DF) of arrhythmia generation for different scenarios of HHD over time.

2. Methods

2.1. Stretch and dilation modeling

To reproduce the elastic response experienced by the tissue during the acute stretch period and the G&R response in a more advanced chronic period, were employed the Hyperelastic constrained mixture model by Bellini et al. [4] and the Mechanobiologically equilibrated constrained mixture (MbeCmm) model by Latorre et al. [5], respectively. Two mathematical models, which by approaching biological structure and function, predict via constitutive relations the homeostatic tendency of cardiac tissue.

From an initial square 3D model (see Figure 1) representing a patch of LA tissue, the two constitutive models were used to estimate the change in dimensions for certain sustained pressure increases, specific for each case study. Given that stretching of the atrium is a nonlinear

function of intra-atrial pressure, elasticity limit of atrial wall is around 12 mmHg pressure. Based on this, to reproduce a particular state of acute stretching, an increase in internal pressure of up to 15 mmHg, i.e., an increase of 200% as to the baseline value, was considered. To reproduce chronic dilation, an increase of 50% and 100% was considered, representing HHD in severe and end-stage phases, respectively.

The following patch dimension values were obtained for each case study, shown in Table 1. The 3D models were adjusted for subsequent simulations of electrical activity.

Table 1. Patch dimensions of each 3D model corresponding to the baseline state (healthy) and the different LA tissue substrates.

	Pressure increase (%)	***Patch dimensions (x,y,z) (cm)***
Healthy	-	5x5x0.3
Acute stretch	200	5.28x5.27x0.27
Severe phase	50	5.47x5.87x0.528
End-stage phase	100	5.56x6.02x0.678

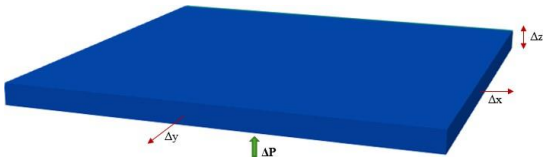

Figure 1. Square 3D model that represents a patch of LA tissue.

2.2. Atrial electrophysiology modeling

To model the LA myocyte electrical activity was employed the Courtemanche-Ramirez-Nattel (CRN) model [6]. The formulation of the potassium-activated acetylcholine current ($I_{K,ACh}$) proposed by Grandi et al. [7] was also included, with [ACh] = 0.005 µM. Additionally, the stretch-activated current (I_{sac}) with Na^+, K^+, and Ca^{2+} contributions was integrated, as proposed by Kuijpers et al. [8].

Scaling factors, shown in Table 2, were applied to the maximum conductances of selected ionic currents in order to adjust this model to the heterogeneities of LA tissue. In addition, tissue with AF-induced electrical remodeling (peAF) was considered as a comparative model for healthy tissue.

Table 2. Scaling factors for fitting CRN model maximum conductances to healthy and peAF LA tissue models.

	G_{CaL}	***G_{Kr}***	***G_{Ks}***	***G_{Kur}***	***G_{K1}***	***G_{Kto}***	***$G_{K,ACh}$***
Healthy	0.9	2	-	-	-	-	-
peAF	0.35	-	2	0.55	2	0.25	2

The reduction of the conduction velocities was considered for cases where tissue has been altered due to electrical or structural remodeling. Diffusion coefficients were modified according to a decrease of 15% in intercellular conductivity for peAF model [9] and to the predicted change in collagen mass fraction by the MbeCmm model for severe phase and end-stage phase models.

Table 3. Conduction velocities and diffusion coefficients of the longitudinal and transverse directions for the different LA tissue substrates.

	Healthy	***peAF***	***Severe phase***	***End-stage phase***
CV_L (cm/s)	63.3	56.96	62.61	62.35
CV_T (cm/s)	36.5	28.82	26.54	22.83
D_L (cm^2/s)	0.115	0.105	0.114	0.122
D_T (cm^2/s)	0.055	0.038	0.028	0.021

2.3. Tissue simulations

All electrophysiological simulations were carried out using the multi-physics finite element solver svFSIplus. These were performed on the different 3D tissue models of adjusted dimensions (see Table 1) with spatial resolutions of 300 µm each.

Six different atrial-tissue models were simulated: healthy, peAF + ↓D_L, acute stretch + SACs, acute stretch + peAF + ↓D_L + SACs, severe phase + ↓D_L and end-stage phase + ↓D_L.

First, the tissues were stabilized employing the S1 protocol, with a train of 5 planar current pulses with an amplitude of twice diastolic threshold and 2-ms (milliseconds) duration, delivered at a Basic Cycle Length (BCL) of 500 ms. Then, a S1-S2 cross-field protocol was used to induce re-entrant activity. The rectangular stimulus S2 was applied in the lower left corner of the tissue after the 5^{th} planar pulse with a minimum coupling interval (CI) determined by the occurrence of the first re-entry. CI was increased with an interval of 1 ms until the end of the re-entrant activity. The width of the VW was determined by the totality of CIs that gave rise to a re-entry activity of at least 1-s (second) duration. For the calculation of the arrhythmia DF, simulations were run for 3 s and only information from the last 2 s was considered.

Action Potential Duration (APD) at the 90% of repolarization (APD_{90}) and Effective Refractory Period (ERP) were also computed for the last pulse of stabilization.

3. Results and discussion

3.1. Acute stretching characterization

Healthy and peAF atrial tissues are the initial stages for the acute stretch characterization. AF-induced electrical remodeling features an electroanatomical substrate that promotes the maintenance of AF, driven by electrophysiological and anatomical alterations that cause a change in ionic channel conductivities and a slowdown in AP conduction. Table 4 provides a summary of the main electrical properties of each substrate, including those observed following a short-term pressure increase over 10 seconds, which induces acute tissue stretching. Figure 2 shows the re-entry waves of these models.

Table 4. APD_{90}, ERP, VW, frequency and re-entries average values for the different LA tissue substrates of study in acute stretching.

	Healthy	***peAF***	***Acute stretch***	***peAF + Acute stretch***
APD$_{90}$ *(ms)*	187	154	192	161
ERP *(ms)*	200	152	232	164
VW *(ms)*	27	41	19	41
Av. reentries	3.83	8.11	3.50	8.08
DF *(Hz)*	6.99	9.13	5.08	8.51

The shortening of APD_{90} and ERP was experienced when considering the peAF electrical remodeling in both healthy control and acute stretch models. Alternatively, the activation of SACs during stretch resulted in diastolic membrane depolarization and prolongation of APD, as observed experimentally [10]. The VW values obtained reveal the greater vulnerability to re-entrant activity in the substrates with AF-induced remodeling as well as in stretching. However, a remarkable reduction in VW is observed in healthy tissue during stretching, which is mainly attributed to alterations in the AP due to the increase in the membrane conductance. The average and frequency values of re-entries reassert the peAF property of sustaining AF activity, as well as acute tissue stretch.

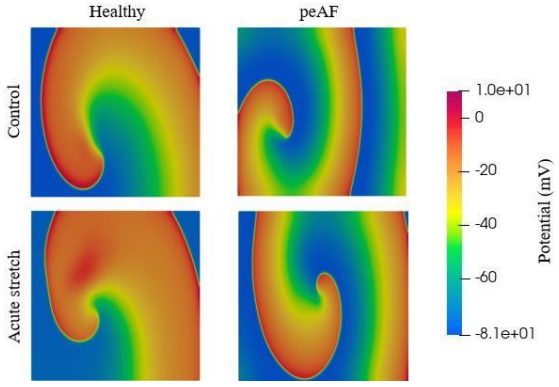

Figure 2. Re-entry waves in healthy, peAF, acute stretch and peAF + acute stretch models.

3.2. Chronic dilation characterization

The degree of tissue thickening, hypertrophy and fibrosis reached in the severe and end-stage phases during the chronic dilation was quantified by running the MbeCmm model in MATLAB. Figure 3 shows the progression of the homeostatic response of the tissue expressed through an exponential mass growth and microstructural remodeling, reflecting as a result the decrease and control of tissue stress. In the severe phase, after reaching a 50% increase in internal pressure, tissue thickness increases in a 76%, associated with an increment in cardiac muscle and collagen mass fractions of 20% and 53.8%, respectively. When 100% increase in pressure is reached, thickness increases by a further 28.41%. The evolution of the Jacobian determinant reflects the change in wall volume given the mass growth in the axial, circumferential and radial directions. In turn, greater hypertrophy and fibrosis is obtained by 2.38% and 25% higher mass fractions of cardiac muscle and collagen, respectively.

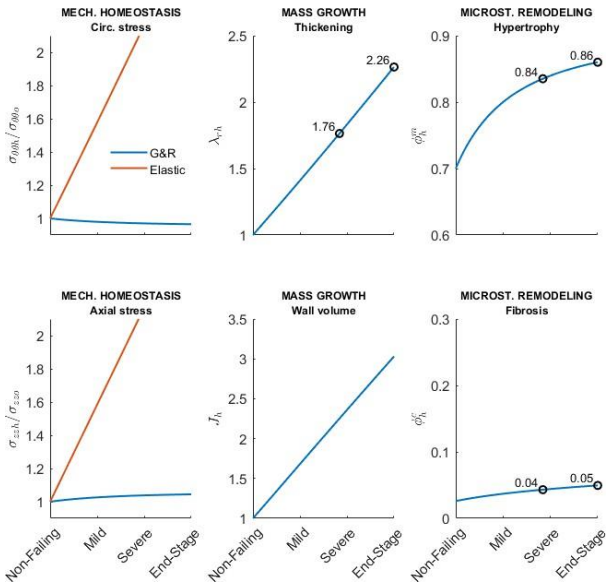

Figure 3. Progression of mass growth and microstructural remodeling from a non-failing to an end-stage state during the process of mechanical homeostasis.

These changes at the structural level led to a slowdown in the conduction velocities and a progressive increase of tissue volume, characteristics that raise the likelihood of the onset and maintenance of fibrillatory activity, as quantified by VW and arrhythmia frequency calculations. Table 5 shows these results for each stage along with the characterization of their APs before arrhythmia induction through APD_{90} and ERP.

Table 5. APD_{90}, ERP, VW, frequency and re-entries average values for the different LA tissue substrates of study in chronic dilation.

	Non-failing	*Severe*	*End-stage*
***APD$_{90}$** (ms)*	187	198	199
***ERP** (ms)*	200	211	212
***VW** (ms)*	27	35	36
Av. reentries	3.83	7	7.05
***DF** (Hz)*	6.99	7.14	7.11

A longer duration of APs is observed as G&R progresses, as shown by the APD_{90} and in turn, an increase in ERP, as expected. Severe phase shows a VW 8 ms longer than the one obtained in the control non-failing phase, with additionally, an average of re-entries significantly higher. In the end-stage phase, a slightly greater tissue susceptibility to antiarrhythmic activity was observed with a 1 ms larger VW. No major difference in the frequency of arrhythmias between substrates was detected; however, remodeled phases result in a more sustained reentrant activity.

3.3. Limitations and future perspectives

By using 3D heart models, this study can be enhanced to provide more accurate results that consider other significant factors such as the complexity of cardiac geometry and fiber directions. Additionally, the complete coupling of the electrical and G&R models provides a more precise representation and enables a more effective analysis.

4. Conclusions

This study addresses the mechanical and electrical mechanisms underlying left atrial dilation, a further step in the research on cardiac tissue response in the various phases of this condition. Our results suggest that, from a healthy non-failing tissue state, the slow process of homeostatic adaptation through G&R (~years) manages to maintain atrial functionality, although accompanied by an increased risk of arrhythmias. Conversely, the acute stretch response (~seconds) modulates multiple current components that minimize this tissue vulnerability to AF. However, tissues undergoing AF-induced remodeling exhibit a higher arrhythmogenic potential which provides prolonged arrhythmia activity and persist under acute stretch conditions. This underscores the significance of employing computational models in the study of LA dilation, both mechanically and electrically, given their implications in the development of AF.

Acknowledgments

This work was supported by the Dirección General de Política Científica de la Generalitat Valenciana PROMETEO/2020/043 and was partially funded by grant PID2022- 140553OB-C41 funded by MICIU/AEI/10.13039/501100011033 and by ERDF/EU. The work of Gavier was supported by the "Programa INVESTIGO 2022 de la Generalitat Valenciana" INVEST/2022/482.

References

[1] R. Yang, X. Zhang, J. Bai, L. Wang, W. Wang, and J. Cai, "Global, regional, and national burden of hypertensive heart disease among older adults in 204 countries and territories between 1990 and 2019: a trend analysis," *Chinese Medical Journal*, vol. 136, no. 20, pp. 2421–2430, Sep. 2023.

[2] C. C. Nwabuo and R. S. Vasan, "Pathophysiology of hypertensive heart disease: beyond left ventricular hypertrophy," *Current Hypertension Reports*, vol. 22, no. 2, Feb. 2020.

[3] T. L. Riemer, E. A. Sobie, and L. Tung, "Stretch-induced changes in arrhythmogenesis and excitability in experimentally based heart cell models," *AJP Heart and Circulatory Physiology*, vol. 275, no. 2, pp. H431–H442, Aug. 1998.

[4] C. Bellini, J. Ferruzzi, S. Roccabianca, E. S. Di Martino, and J. D. Humphrey, "A microstructurally motivated model of arterial wall mechanics with mechanobiological implications," *Annals of Biomedical Engineering*, vol. 42, no. 3, pp. 488–502, Nov. 2013.

[5] M. Latorre and J. D. Humphrey, "Fast, rate-independent, finite element implementation of a 3d constrained mixture model of soft tissue growth and remodeling," *Computer Methods in Applied Mechanics and Engineering*, vol. 368, p. 113156, Aug. 2020.

[6] M. Courtemanche, R. J. Ramirez, and S. Nattel, "Ionic mechanisms underlying human atrial action potential properties: insights from a mathematical model," *AJP Heart and Circulatory Physiology*, vol. 275, no. 1, pp. H301–H321, Jul. 1998.

[7] E. Grandi *et al.*, "Human atrial action potential and ca2+ model," *Circulation Research*, vol. 109, no. 9, pp. 1055–1066, Oct. 2011.

[8] N. H. L. Kuijpers, H. M. M. T. Eikelder, P. H. M. Bovendeerd, S. Verheule, T. Arts, and P. a. J. Hilbers, "Mechanoelectric feedback leads to conduction slowing and block in acutely dilated atria: a modeling study of cardiac electromechanics," *AJP Heart and Circulatory Physiology*, vol. 292, no. 6, pp. H2832–H2853, Jun. 2007.

[9] L. Martinez-Mateu "Mapping of the electrical activity of human atria multiscale modelling and simulations", 2018. (Doctoral dissertation, Universitat Politècnica de València).

[10] J. B. Youm *et al.*, "Role of stretch-activated channels on the stretch-induced changes of rat atrial myocytes," *Progress in Biophysics and Molecular Biology*, vol. 90, no. 1–3, pp. 186–206, Jan. 2006.

Address for correspondence:

Javier Saiz.
Centro de Investigación e Innovación en Bioingeniería (Ci2B), Universitat Politècnica de València (UPV) Camino de Vera s/n, 46022 Valencia, Spain.
jsaiz@ci2b.upv.es